nature neuroscience

Neural population partitioning and a concurrent brain-machine interface for sequential motor function

Maryam M Shanechi[1–3], Rollin C Hu[2,3], Marissa Powers[2], Gregory W Wornell[1], Emery N Brown[3–7] & Ziv M Williams[2,3]

Although brain-machine interfaces (BMIs) have focused largely on performing single-targeted movements, many natural tasks involve planning a complete sequence of such movements before execution. For these tasks, a BMI that can concurrently decode the full planned sequence before its execution may also consider the higher-level goal of the task to reformulate and perform it more effectively. Using population-wide modeling, we discovered two distinct subpopulations of neurons in the rhesus monkey premotor cortex that allow two planned targets of a sequential movement to be simultaneously held in working memory without degradation. Such marked stability occurred because each subpopulation encoded either only currently held or only newly added target information irrespective of the exact sequence. On the basis of these findings, we developed a BMI that concurrently decodes a full motor sequence in advance of movement and can then accurately execute it as desired.

An important motivation for the design of BMIs so far has been their potential ability to restore lost motor function in individuals with neurological injury or disease (for example, because of motor paralysis or stroke). In such cases, the envisioned role of the BMI is to decode the intended movement from neural activity in the relevant areas of the brain and use this information to control an affected limb, prosthetic or other device.

The design of such BMIs has received considerable attention in recent years[1–18]. Work so far has focused principally on achieving the motor goal in tasks that involve single-targeted movements, such as moving a cursor on a display to an individual target location. These BMIs can decode the continuous trajectory of one- to three-dimensional movement (including a grasp in some studies)[1–14], the intended target location[15,16] or both the target and trajectory jointly using approaches such as optimal feedback control[17,18]. However, in many natural tasks—such as playing a succession of notes on a piano—the goal is more complex, and the motor plan for achieving it can be considered as a complete sequence of such simpler plan elements to be executed in order.

Our focus is on the design of BMIs that can achieve the goal of these sequential motor plans. Planned sequential behavior is a fundamental motor process in which all targets of a movement sequence are planned ahead of its initiation. Hence, a BMI for performing such behavior would allow a person to plan a full motor sequence ahead of execution. For example, when picking up a cup and bringing it to one's lips, a person normally formulates the complete motor plan before its execution, as opposed to planning and performing each of its elements individually and separately. Therefore, the objective of such a BMI would be to perform the sequential behavior by decoding all elements of the sequence concurrently and in advance of movement, thus requiring the consideration of a concurrent architecture. This BMI functionality is distinct from that in prior BMIs that decode and execute individual single-targeted movements one by one and, hence, have a sequential BMI architecture[1–18].

In addition to simultaneously decoding a motor sequence in advance, a concurrent architecture could also allow the BMI to consider the overall motor goal of the task at a higher level. This is a result of the BMI having information about all the motor-plan elements at once and in advance of execution. Hence, one prospective BMI capability would be to consider all elements of the sequence concurrently, before action, to determine ways to perform the task more effectively. For example, the BMI might determine a way to accomplish the task more quickly or more efficiently (within any physical constraints that might exist). Alternatively, on the basis of additional sensor inputs, the BMI might determine that the planned sequence of movements would result in an accident with an obstacle and thus modify the execution of the task to avoid such an accident (see Discussion).

The development of BMIs that can perform and potentially execute sequential motor function more effectively in this way will require substantial technological innovations. But as a key initial step, it is necessary to consider a concurrent BMI architecture in which the elements of a planned motor task are decoded in parallel (at once), which is in contrast to the serial process of a sequential BMI. Hence, the feasibility of such BMIs hinges on the degree to which the elements

[1]Department of Electrical Engineering and Computer Science, Massachusetts Institute of Technology, Cambridge, Massachusetts, USA. [2]Department of Neurosurgery, Massachusetts General Hospital, Boston, Massachusetts, USA. [3]Harvard Medical School, Boston, Massachusetts, USA. [4]Department of Brain and Cognitive Sciences, Massachusetts Institute of Technology, Cambridge, Massachusetts, USA. [5]Department of Anesthesia, Critical Care and Pain Medicine, Massachusetts General Hospital, Boston, Massachusetts, USA. [6]Institute for Medical Engineering and Science, Massachusetts Institute of Technology, Cambridge, Massachusetts, USA. [7]Harvard-MIT Health Sciences and Technology Program, Massachusetts Institute of Technology, Cambridge, Massachusetts, USA. Correspondence should be addressed to Z.M.W. (zwilliams@partners.org).

Received 27 June; accepted 2 October; published online 11 November 2012; doi:10.1038/nn.3250

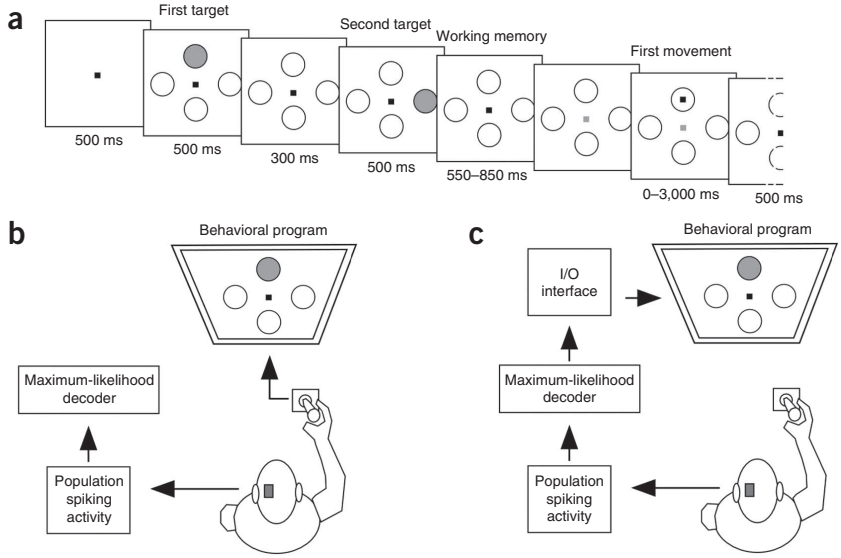

Figure 1 Task design and experimental setup. (**a**) Schematic illustration of a standard dual-target task over a single trial. Task events and their timings are shown over a single trial from left to right. The right end, in which the second movement is depicted, is truncated to conserve space. Decoding analyses are performed during the 500-ms blank-screen interval after presentation of the second target. (**b**) Experimental setup for the standard training sessions. (**c**) Experimental setup for the BMI sessions. I/O, input/output.

of a motor-plan sequence can, in fact, be decoded concurrently. This was the starting point for our research.

Prior work has demonstrated that individual neurons in the premotor cortex of primates have selective responses to planned single-targeted movements before their initiation and that such responses often remain sustained during working memory until movement execution[19–26]. Such responses have been successfully exploited in the design of BMIs for single-target tasks[15,16,18]. In comparison, the neural encoding of tasks requiring a full sequence of planned targeted movements to be formulated before execution is less well understood, and the design of real-time BMIs that can concurrently decode and then execute such sequential motor plans remains unexplored. Prior work has shown that an individual neuron can have a response that is selective to one or more elements of a sequential motor plan[27–41] (see Discussion). However, little is known regarding how information about multiple elements of a sequential motor plan (for example, the planned targets of a sequential movement) is simultaneously distributed across the whole premotor population during working memory and whether these plan elements can be accurately decoded from the neural population in a concurrent manner. More importantly, it is necessary to determine whether adding information about the elements of the motor plan, in sequence, to working memory affects the integrity of information about the plan elements that are already held and how it affects their neural encoding. In addition, it is necessary to assess robustness: whether a BMI that is limited to recording from relatively small numbers of neurons is able to achieve sufficient and consistent decoding accuracy.

We found that sequential motor plans can be decoded simultaneously, accurately, robustly and in advance of movement from the neural activity in the premotor cortex of monkeys. In addition, our results reveal a remarkably structured encoding mechanism that is used by the premotor populations for these sequential plans and that, in turn, allows for their accurate and concurrent decoding. On the basis of these findings, we developed and implemented a real-time BMI that can concurrently decode a dual sequence of motor targets and then execute them as desired.

RESULTS

We trained two adult male rhesus monkeys to perform a task in which two targets were presented in sequence on a computer display. Each of the targets could randomly take on one of four possible spatial locations (up, down, left or right). Repeated locations were precluded, so there were a total of 12 possible combinations (sequences) of two consecutive distinct target locations. After a blank-screen variable delay, a 'go' cue appeared that directed the monkeys to sequentially move a cursor from the center of the screen to each of the two remembered targets in order (referred to as a dual-target task; **Fig. 1**). We defined the working memory period as the 500-ms blank-screen interval after the presentation of the second target and before the earliest possible 'go' cue. Therefore, the task here was a working-memory task in which the monkeys were required to serially add to working memory two randomly selected target locations in each trial and then simultaneously retain them in working memory before execution (**Fig. 1a**).

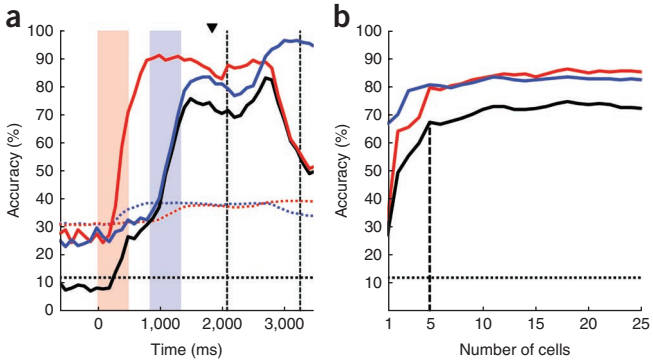

Figure 2 Population decoding accuracy for a selected session. (**a**) Population decoding accuracy over time for the first target (red curve), second target (blue curve) and full sequence (black curve). Each point on the curves indicates the decoding accuracy for the population over the preceding 500-ms window. The time at zero is aligned to the start of first target presentation. The pink and blue vertical bars indicate the times during which the first and second targets were presented, respectively. The left and right vertical dashed black lines indicate the mean times at which the first and second go cues were given, respectively. The arrowhead indicates the time point of decoding for the preceding working memory period (0–500 ms from the end of the second target presentation). The dotted lines indicate the 99% chance upper confidence bounds for the first target, second target and sequence (out of 12 possibilities), with the same respective color scheme used above (see also **Supplementary Modeling**). (**b**) Number of cells sufficient to reach the decoding accuracy asymptote during the working memory period for the same session. The first target (red curve), second target (blue curve) and sequence (black curve) accuracies are shown as a function of the cumulative number of cells in descending order of single-cell sequence accuracy. The number of cells needed to reach over 90% of the population accuracy is indicated by the vertical dashed line.

We recorded multiple-unit responses from the premotor cortex as the primates performed this task. Specifically, we recorded 281 well-isolated single neurons from the supplementary motor area and dorsal premotor cortex (PMd) over 11 sessions for an average of 26 ± 6 cells (mean ± s.d.) per recording session (note that some of these cells may not be distinct across the different sessions). We fitted inhomogeneous Poisson models to each neuron's spiking activity using an expectation-maximization algorithm[42] (Online Methods and **Supplementary Modeling**). We used these models and a maximum-likelihood decoder to quantify the probabilities that groups of neurons could correctly identify the first and second targets on a trial-by-trial basis during the working memory period (using a leave-one-out cross-validation; Online Methods). We used decoding accuracy as our measure of the amount of information encoded by a population of neurons about each target. Specifically, for an individual (first or second) target, we measured the percentage of trials in which the maximum-likelihood decoder correctly predicted the respective target from that population's activity. Likewise, we measured the amount of information encoded about the full sequence as the percentage of trials in which both targets were correctly decoded.

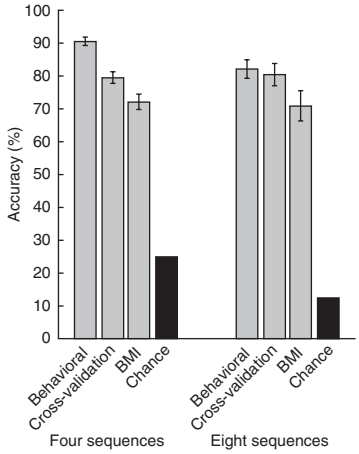

Figure 3 Decoding accuracies in BMI trials. The gray bars indicate the monkeys' average behavioral accuracy, maximum-likelihood cross-validation accuracy on the training data and real-time BMI accuracy, with the corresponding s.e.m. shown. The black bars indicate chance level accuracies. Performances using four sequences are shown on the left, and performances using eight sequences are shown on the right.

Accurate, robust, and concurrent encoding of the sequence

We found that neural population activity within the premotor cortex accurately encoded the location of both targets during the working memory period. During this period, the population correctly encoded the first and second targets in 85% and 82% of the trials in the session with the highest encoding accuracies, respectively. When considering all 12 possible target combinations, the population encoded both targets correctly in 72% of the trials in this session, which included a total of 285 dual-target trials (**Fig. 2a**). Across all sessions tested, the population correctly encoded the first and second targets, on average, in 76 ± 11% (mean ± s.d.) and 56 ± 17% of trials, respectively, both of which are significantly above the percentage expected by chance (one-sided Z test, $P < 10^{-15}$; **Supplementary Fig. 1a**). Also, the population encoded both targets correctly on average on 45 ± 12% of the trials across all sessions, which was also far higher than expected by chance at 1/12 or ~8% (one-sided Z test, $P < 10^{-15}$). These results were consistent across the two monkeys ($P < 10^{-15}$ for both; **Supplementary Fig. 2**).

This accurate encoding of the motor sequence was also robust. Only a small number of cells were needed to decode the target sequence with high accuracy. When performing the decoding analysis over all trials, which used all 12 possible target combinations, only 29% of the population (7.5 cells) was needed, on average, to achieve higher than 90% of the population sequence accuracy (**Fig. 2b** and Online Methods). When performing the decoding analysis over subsets of all trials that used only four or eight target combinations, population sequence accuracies in the best session were as high as 93% and 80%, respectively. In these trials, decoding from only two and four cells, respectively, was sufficient to achieve higher than 90% of these population sequence accuracies.

Real-time concurrent BMI for sequential movement execution

Motivated by the observation that both targets can be concurrently and accurately decoded from the responses of relatively few neurons in the premotor cortex, we developed a real-time BMI that was capable of predicting both targets simultaneously before the monkey's motor response and then executing the targeted movements. In the associated experiments, we recorded a mean of 20 ± 2 cells per session from the premotor cortex of the same monkeys described above. We fitted Poisson models to the neural population activity during the working memory period before the go cue (Online Methods and **Supplementary Fig. 1b**) as the primates rehearsed a subset of target combinations that included either four or eight possible sequences over an average of 26 ± 2 (mean ± s.d.) training trials per sequence (**Fig. 1b**). We chose to use either four or eight sequences in the BMI experiments to obtain sufficient training and real-time trials per session.

Using the Poisson models, the sequence decoding accuracies for the set of four and eight sequences in these training sessions (found using

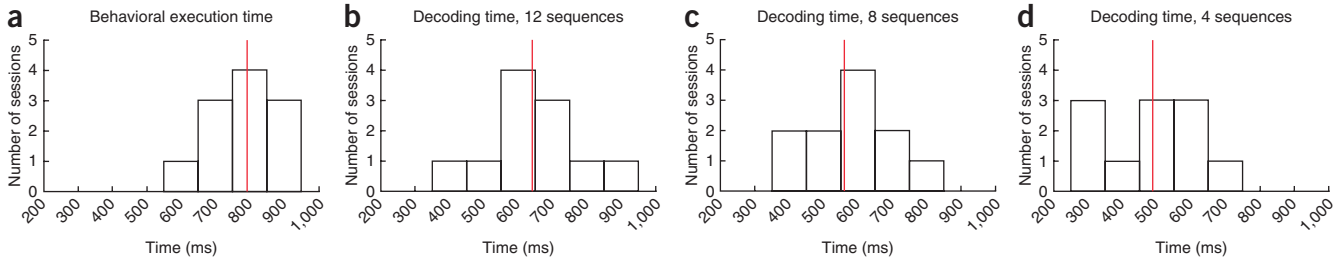

Figure 4 Decoding and behavioral performance times. (**a**) Histogram of the total times it took the monkeys to behaviorally react to the two go cues and reach the two targets (excluding any task delays and the time required to move from the targets to the center). (**b**–**d**) Histograms of the times required for the decoding accuracy to reach 90% asymptotic accuracy from the time of second target presentation for 12, 8 and 4 sequences. The red lines indicate the mean times for each histogram.

leave-one-out cross-validation) were 79 ± 2% and 80 ± 3% (mean ± s.e.m.; one-sided Z test, $P < 10^{-15}$), respectively. After training, the primates performed the same task as before but with the cursor now being sequentially positioned by the BMI on the targets decoded from the recorded neuronal activity during the single preceding working memory period (**Fig. 1c** and Online Methods). We set the BMI-generated cursor movements to occur immediately after the presentation of the go cue and selected the added delays to match the reaction times that the monkeys normally experienced when moving the cursor themselves after the go cue (note that cursor movements could be generated without the added delays, if desired).

Both monkeys performed a total of 459 trials on the four-sequence set, and one of the monkeys performed 110 trials on the eight-sequence set using the real-time BMI. The sequence accuracies for the set of four and eight sequences were 72 ± 2% and 71 ± 4%, respectively, both of which were significantly above the percentages expected by chance (mean ± s.e.m.; one-sided Z test, $P < 10^{-15}$). Both the training and real-time BMI accuracies were similar and significantly above those expected by chance across the two monkeys (one-sided Z test, $P < 10^{-15}$ for both.) (For the four sequence sets, the first monkey had a BMI accuracy of 69 ± 3% and a training session accuracy of 77 ± 2%, and the second monkey had a BMI accuracy of 75 ± 3% and a training session accuracy of 82 ± 2%). Sequence accuracies using the BMI were also close to the cross-validated sequence accuracies during the training sessions when taking into account the primates' natural error rates during the standard task (**Fig. 3**). In fact, the 95% confidence

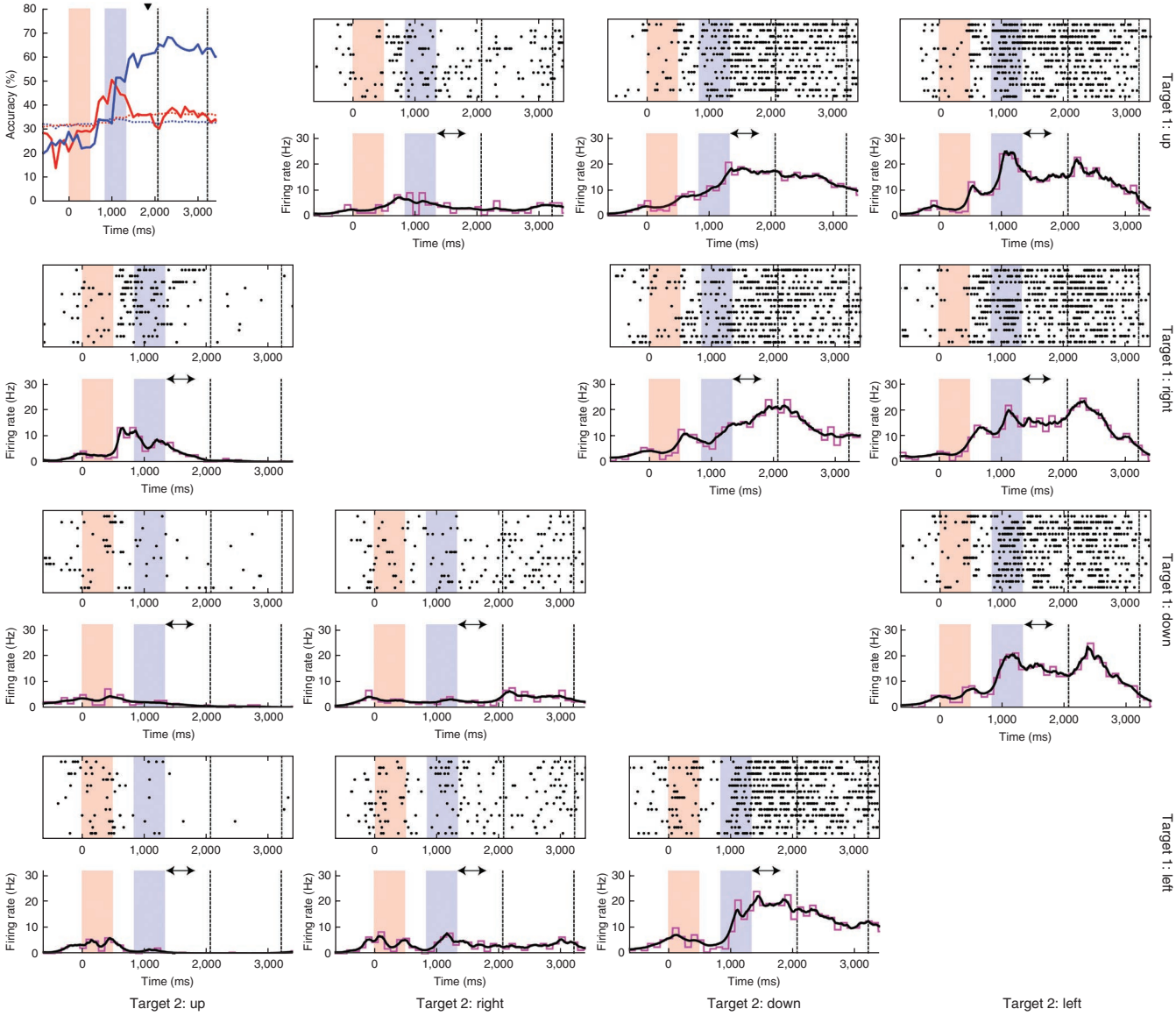

Figure 5 Example of a second (added) target selective neuron. The graph in the upper left corner shows the first and second target accuracies of the cell as a function of time into the trial. The vertical bars and dashed lines and their timings, as well as the color scheme of the curves, follow the same convention as in **Figure 2**. In all other pairs of graphs, the top graph corresponds to a different sequence of movements, with each row illustrating the spiking activity during a single trial, and the black dots indicate the spike times. The bottom graph indicates the corresponding mean firing rate estimates using the expectation-maximization procedure (black curve) and the corresponding peristimulus time histogram (magenta curve). The arrowhead indicates the working memory period. The graphs in the same row correspond to sequences with the same first target location. The graphs in the same column correspond to sequences with the same second target location. Repeated target locations were not used in the sequences, and, hence, there are three subfigures per row and per column (**Supplementary Figs. 3** and **4**).

bounds for the two accuracies overlapped (72 ± 4% and 73 ± 3%, and 71 ± 8% and 66 ± 6% for the sets of four and eight sequences, respectively; Online Methods). These results established that two planned elements (the two intended sequential targets of movement) could be simultaneously predicted in advance of movement and then executed by a real-time BMI with high accuracy.

We also examined the time required by the concurrent decoder to decode the sequence. We found that the sequence decoding accuracy for the set of 4, 8 and 12 sequences reached 90% of the maximum asymptotic accuracy possible, on average, 488 ± 135 ms, 561 ± 119 ms and 641 ± 121 ms, respectively, after the initial presentation of the second target (**Fig. 4**). When performing the motor sequence, the minimum total time it took for the monkeys to both react to the two go cues and reach the two targets was, on average, 791 ± 93 ms (the sum of the two reaction times plus the two center-to-target movement times; **Fig. 4**).

Population encoding reveals a new partitioning mechanism

Observing that both target locations could be accurately and concurrently predicted from the neural population responses, we further examined the spatial and temporal structure of their encoding. In particular, we investigated how neurons within the premotor cortex were able to add new information about the second target to working memory without compromising the integrity of information about the first target that was already being held. To do so, we used a decoding approach that measures the amount of information held about the identity of each planned target in the sequence by considering all sequence combinations collectively.

We found that most cells encoded significant information about only the first (currently held) or only the second (newly added) target during the working memory period (one-sided Z test, $P < 0.01$). Moreover, this partitioning was present across all target locations and sequences (meaning that responses were not sequence specific) and remained stable throughout all recordings per day. Of the 281 neurons recorded in all sessions, 46% had a target accuracy that was significantly higher than expected by chance for at least one of the two targets during the working memory period (one-sided Z test, $P < 0.01$). Of these, 68% encoded significant information about only the first currently held target (**Supplementary Fig. 3**), and 23% encoded significant information about only the second added target (one-sided Z test, $P < 0.01$; **Fig. 5**). The percentage of cells that encoded significant information about both targets was only 9% (one-sided Z test, $P < 0.01$; note that we performed a Bonferroni correction for multiple comparisons for all comparisons; **Supplementary Fig. 4**), and even among these cells, most had target accuracies that were much closer to that of one of the two subpopulations of cells that significantly encoded only one target (**Fig. 6** and **Supplementary Fig. 5**). These results revealed a highly significant divergence in the amount of information encoded by the two subpopulations of neurons about the two targets (random permutation test, $P < 10^{-15}$; **Supplementary Modeling** and **Supplementary Fig. 6**). Moreover, we examined the relation between the activity of each of the two subpopulations to upcoming motor behavior and found that each subpopulation was only predictive of whether the first or second upcoming movement would be performed correctly or incorrectly (that is, resulting in a behavioral error) by the primates after the go cue (one-sided Z test, $P < 10^{-15}$).

These results demonstrate that during the working memory period, most neurons were not selective to a specific sequence or simply a spatial location. Rather, they were partitioned into two disjoint subpopulations, one encoding only the identity of the currently held (first) target and one encoding only the identity of the newly added (second) target within the sequence, regardless of the specific sequence (see **Supplementary Fig. 7** for a comparison to sequence-specific selectivity found in prior works[28–31,41,43]).

The observed partitioning during working memory was not related to limb movement or simple visual-related responses. No visual cues were presented during the working memory period, and any movement before the go cue terminated the trial. This lack of relationship was also suggested by the partitioning mechanism itself, because if the activity was the result of targeted limb movement, then all cells would only reflect the direction of this single target. In addition, the electromyography activity during the working memory period was not predictive of the first movement direction (one-sided Z test, $P = 0.14$) but was predictive of this direction during the first movement period after the go cue (one-sided Z test, $P = 0.01$). In an additional set of analyses, we also found that encoding of the second target was not conditioned on the location of the first target and vice versa (**Supplementary Fig. 8**).

Effect of adding information to working memory

To further examine how adding a new target to working memory affected the integrity of the currently held target, we disambiguated the process of holding information in working memory from that of adding information to it. We obtained the results from sessions in which the monkeys performed the standard dual-target trials (as before) but also performed single-target trials, in a randomly interleaved fashion (Online Methods). Unlike in dual-target trials,

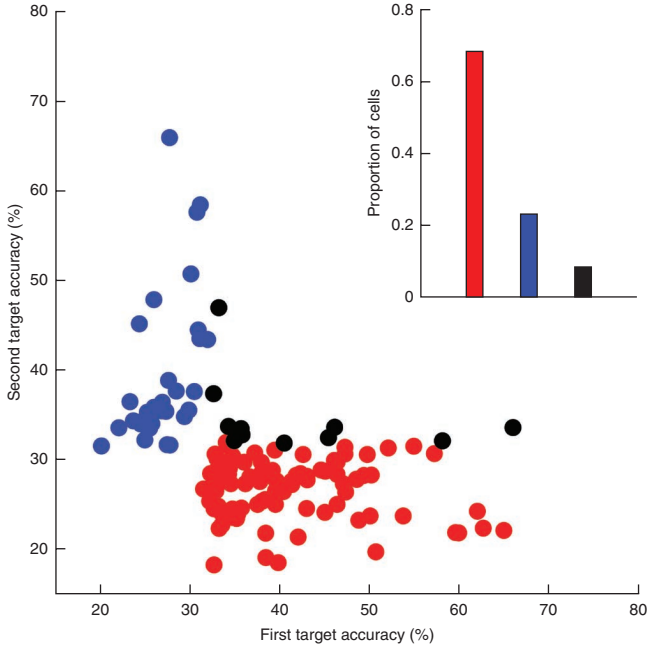

Figure 6 Distribution of first and second target information across the population. Scatter plot of the first and second target accuracies for the 129 cells that encoded significant information about at least one target during the working memory period (across 12 sequences). The statistical significance of the target accuracies was tested here at the $\alpha = 0.01$ level (**Supplementary Fig. 6**). Red points indicate cells that encoded significant information about only the first target, blue points indicate those that encoded significant information about only the second target, and black points indicate those that encoded significant information about both targets. The inset indicates the proportion of cells that encoded significant information about only the first, only the second or both targets during the working memory period with the same color scheme as described above.

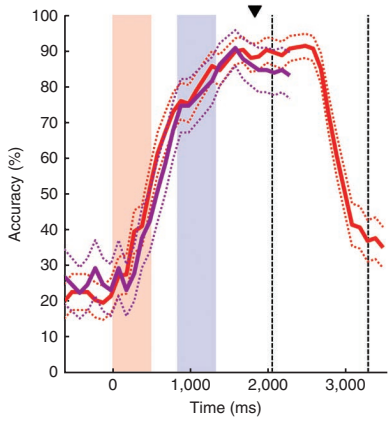

Figure 7 The effect of adding information to working memory. In an interleaved session, the population decoding accuracy for the first target in dual-target trials is shown in red, and the population decoding accuracy for the first target in single-target trials is shown in magenta. Each point on the curves indicates the decoding accuracy over the preceding 500-ms window. Dotted curves indicate the 95% confidence bounds for accuracy of each curve (rather than chance level). The vertical pink bar indicates the time during which the first target was presented. The vertical blue bar indicates the time during which the second target was or was not shown depending on the trial type. The arrowhead indicates the time point corresponding to the decoding accuracy of the preceding working memory period (data are presented as in **Fig. 2**).

in single-target trials only the first target was presented, and the second target presentation period was replaced with a blank-screen period of the same duration. The task timing was otherwise unchanged compared to the dual-target task.

We found that adding information about the second target location to working memory did not incur loss of information about the first target location. Of the cells that encoded significant information about the first target during working memory in single-target trials (one-sided Z test, $P < 0.01$), most (74%) provided the same level of accuracy in decoding the first target during working memory in dual-target trials despite the addition of a second target (χ^2 test, $P > 0.05$). Moreover, for the whole population, there was no significant difference in first target accuracy during the working memory period when comparing dual-target and single-target trials across sessions (Wilcoxon signed-rank test, $P = 0.69$; **Fig. 7**). These results demonstrate that the subpopulation encoding the first target and the responses of that subpopulation remained largely unchanged when the second target was added to working memory, and therefore the addition of information about the second target did not comprise the integrity of information already held about the first target. It is important to emphasize here that this task involved serially adding to working memory two randomly selected target locations in each trial and then simultaneously holding them in working memory before execution. Such a task is distinct from memory-guided tasks in which the same motor sequence is repeatedly performed from memory after learning and visually guided tasks in which movements are serially cued and executed one by one[29–31,41,43].

In a control analysis, we also examined whether neuronal encoding of the first target was affected by the number of targets presented per trial in a single session (one target compared to two sequentially presented targets) by having one monkey perform only single-target trials. Comparing these single-target–only sessions with sessions in which we interleaved single-target trials with dual-target trials on the same day, we found no significant difference between the population decoding accuracies of the first target in single-target trials between the two session types (χ^2 test, $P > 0.15$; **Supplementary Fig. 9**).

Finally, although implicit in the preceding results, it should be emphasized that as the pair of presented target locations varied over the hundreds of trials typical of a given day's session, most neurons remained dedicated to encoding only the first (currently held) or second (added) target. For the two subpopulations of cells that encoded significant information about the first or second targets alone, most (89%) provided substantially the same level of accuracy in decoding their respective targets in the first and second halves of the recording session (χ^2 test, $P > 0.05$; the sessions included 263 ± 36 (mean ± s.d.) dual-target trials on average). Also, the sequence decoding accuracy (across all 12 sequences) of the entire population did not change over time between the first and second halves of the sessions (Wilcoxon signed-rank test, $P = 0.37$). Therefore, the partitioned premotor subpopulations seemed to be physiologically dedicated to encoding either the first or second target added to working memory. Inherently, the neural decoding in our BMI exploited this stability of the two constituent subpopulations to achieve sustainable performance.

DISCUSSION

The purpose of the present study was to examine how multiple planned targets of sequential movement are concurrently encoded as a population by premotor neurons during working memory and determine whether the activity recorded simultaneously from multiple single neurons can be used to concurrently and accurately decode the complete motor-plan sequence in advance of movement and in real time. We used three methodological approaches to investigate these questions. First, we simultaneously recorded the activity of multiple cells across the whole premotor population. Second, we used an interleaved dual-target and single-target task to dissociate the dynamic process of maintaining target-related information in working memory from that of adding new information to it. Third, we used a maximum-likelihood decoding approach that allowed us to define an accuracy measure for the amount of information that is concurrently encoded about planned motor sequences and examine the spatiotemporal distribution of information across the whole population.

A neural partitioning mechanism

Our results reveal a new functional structure within the premotor cortex that allowed for accurate and concurrent decoding of two planned motor targets across multiple spatial locations. We found that during working memory, premotor populations are partitioned largely into two fundamentally disjoint subpopulations of cells: one dedicated to encoding only the currently held (first) target and one dedicated to encoding only the newly added (second) target, irrespective of the specific sequence. Moreover, although the two target locations changed from trial to trial, the two encoding subpopulations did not. Notably, the subpopulation dedicated to encoding the first target and the responses of that subpopulation remained largely unchanged when the second target was added to working memory, and therefore the process of adding information did not compromise the integrity of the existing information (across all target locations). Also, only a small number of neurons was sufficient to accurately predict the location of both targets, making the decoding of such information highly robust.

Prior work has shown that individual premotor neurons have selective responses to single-targeted movements before their initiation[19–26]. It has also been shown that PMd neurons can be selective to the location of multiple target choices for a single-targeted movement

before a final selection is made[44] or can represent combined information about the target and the body part to be used for a single-targeted movement[45–47]. When performing a planned sequential movement, prior studies have demonstrated that individual neurons within areas such as the parietal, premotor or prefrontal cortex can have selective responses to a sequential motor plan[27–41,43,48]. Some neurons (often a relatively small fraction) show increased activity for a specific combination of movements (for example, a push followed by a pull of a manipulandum) during a preceding delay, suggesting that they encode information about more than one motor-plan element at a time[28–31,37,41,43]. Other cells have also been found to have selective responses during movement itself, with increased activity before performing a particular movement (for example, a push) only when it follows another specific movement (for example, a pull) in sequence[29,31,43], or before a movement only if it has a particular order in the sequence[31,43]. What has remained unclear, however, is how information about individual elements of such sequential plans is simultaneously distributed across the whole population during working memory and whether and how the process of adding new information about an element to working memory affects the integrity of information already held and its neural encoding.

Although a major focus of this study was to investigate the encoding structure of premotor populations during the working memory period, we found that, consistent with prior studies[29,31,43], neurons often altered the degree to which they encoded information about the two targets across different time points during the task. Some cells, for example, encoded no information about the second target during the working memory period but encoded significant information about the second target during the second movement itself (**Supplementary Fig. 5a**). Such shifts in activity may reflect the dynamic role premotor neurons have in processing, maintaining and then executing motor plans in combination with other motor cortical areas.

Another question arising from the study is how information encoded by premotor neurons is related to the later execution of the sequential task. We found that the subpopulation of cells that predominantly encoded information about the first target was only predictive of whether the primates would perform the first upcoming movement correctly or incorrectly, and this was similarly true for the second subpopulation. This therefore suggests that the 'partitioning strategy' revealed here was ultimately used to direct upcoming sequential motor behavior. In terms of the small number of cells that encoded information about both targets, it is interesting to speculate whether they may provide an important 'bridge' between distinct motor-plan elements or a higher conceptual representation of specific motor combinations not provided by the other subpopulations of neurons.

A concurrent BMI for planned sequential motor behavior

We exploited the simultaneous encoding and neural partitioning mechanism observed in these experiments to develop a new BMI functionality for the performance of planned sequential motor behavior. This is a fundamental behavior in which all targets of a movement sequence are planned ahead of its initiation and is largely distinct from behaviors involving the performance of independent single-targeted movements. The BMI functionality takes advantage of the concurrent encoding of a sequential motor plan in the premotor cortex, allowing it to determine all elements of the sequence simultaneously, upfront and in advance of movement.

In addition, because the full motor plan is simultaneously decoded upfront and in advance of movement, the higher-level goal of the task can, in principle, also be analyzed before execution, and the motor plan can be reformulated accordingly. This could allow for the prospective design of BMIs that can perform a sequential motor task more effectively, for example, more quickly, more flexibly or more efficiently than originally conceived. Such a BMI may, for example, alter the order in which the elements of the motor sequence are executed depending on rapid or unpredictable changes in the environment (for example, to avoid unanticipated obstacles) or correct the original sequence on the basis of the performance metrics of the task (for example, proactively changing a sequence of letters on the basis of spelling rules). As a simple but illustrative example of such a prospective capability (in the context of our experiments and using a relatively small number of recorded neurons), we demonstrate that we could accurately decode the full sequence of two targets in a very short time period after target presentation (**Figs. 3** and **4**). Taken together, we demonstrate a concurrent BMI that allows for the performance of a sequential motor behavior that is in line with how it is naturally planned and executed. Moreover, because information about all elements of the sequence is known ahead of execution, considering such concurrent decoding provides the future prospect of designing BMIs that can perform such tasks more effectively.

METHODS

Methods and any associated references are available in the online version of the paper.

Note: Supplementary information is available in the online version of the paper.

ACKNOWLEDGMENTS

R.C.H. is funded by the Neuroscience Research and Education Foundation, E.N.B. is funded by US National Institutes of Health (NIH) DP1 OD003646, and Z.M.W. is funded by NIH 5R01-HD059852, a Presidential Early Career Award for Scientists and Engineers and the Whitehall Foundation.

AUTHOR CONTRIBUTIONS

M.M.S. developed the BMI real-time decoder, conceived and performed the computational analysis, assisted with animal recordings and wrote the manuscript. R.C.H. and M.P. assisted with animal training and recordings. G.W.W. and E.N.B. were involved in the computational methodological development and writing of the manuscript. Z.M.W. conceived and designed the study, developed the BMI system, performed the animal training and recordings, helped implement the computational models and wrote the manuscript.

COMPETING FINANCIAL INTERESTS

The authors declare no competing financial interests.

Published online at http://www.nature.com/doifinder/10.1038/nn.3250.
Reprints and permissions information is available online at http://www.nature.com/reprints/index.html.

1. Chapin, J.K., Moxon, K.A., Markowitz, R.S. & Nicolelis, M.A.L. Real-time control of a robot arm using simultaneously recorded neurons in the motor cortex. *Nat. Neurosci.* **2**, 664–670 (1999).
2. Wessberg, J. *et al.* Real-time prediction of hand trajectory by ensembles of cortical neurons in primates. *Nature* **408**, 361–365 (2000).
3. Serruya, M.D., Hatsopoulos, N.G., Paninski, L., Fellows, M.R. & Donoghue, J.P. Instant neural control of a movement signal. *Nature* **416**, 141–142 (2002).
4. Hochberg, L.R. *et al.* Neuronal ensemble control of prosthetic devices by a human with tetraplegia. *Nature* **442**, 164–171 (2006).
5. Carmena, J.M. *et al.* Learning to control a brain-machine interface for reaching and grasping by primates. *PLoS Biol.* **1**, e42 (2003).
6. Taylor, D.M., Tillery, S.I.H. & Schwartz, A.B. Direct cortical control of 3D neuroprosthetic devices. *Science* **296**, 1829–1832 (2002).
7. Ganguly, K. & Carmena, J.M. Emergence of a stable cortical map for neuroprosthetic control. *PLoS Biol.* **7**, e1000153 (2009).
8. Wolpaw, J.R. & McFarland, D.J. Control of a two-dimensional movement signal by a noninvasive brain-computer interface in humans. *Proc. Natl. Acad. Sci. USA* **101**, 17849–17854 (2004).
9. Velliste, M., Perel, S., Spalding, M.C., Whitford, A.S. & Schwartz, A.B. Cortical control of a prosthetic arm for self-feeding. *Nature* **453**, 1098–1101 (2008).
10. Moritz, C.T., Perlmutter, S.I. & Fetz, E.E. Direct control of paralysed muscles by cortical neurons. *Nature* **456**, 639–642 (2008).

11. Mulliken, G.H., Musallam, S. & Andersen, R.A. Decoding trajectories from posterior parietal cortex ensembles. *J. Neurosci.* **28**, 12913–12926 (2008).
12. Kim, S.-P., Simeral, J.D., Hochberg, L.R., Donoghue, J.P. & Black, M.J. Neural control of computer cursor velocity by decoding motor cortical spiking activity in humans with tetraplegia. *J. Neural Eng.* **5**, 455–476 (2008).
13. Li, Z. *et al.* Unscented Kalman filter for brain-machine interfaces. *PLoS ONE* **4**, e6243 (2009).
14. Chase, S.M., Schwartz, A.B. & Kass, R.E. Bias, optimal linear estimation, and the differences between open-loop simulation and closed-loop performance of spiking-based brain-computer interface algorithms. *Neural Netw.* **22**, 1203–1213 (2009).
15. Musallam, S., Corneil, B.D., Greger, B., Scherberger, H. & Andersen, R.A. Cognitive control signals for neural prosthetics. *Science* **305**, 258–262 (2004).
16. Santhanam, G., Ryu, S.I., Yu, B.M., Afshar, A. & Shenoy, K.V. A high-performance brain-computer interface. *Nature* **442**, 195–198 (2006).
17. Shanechi, M.M., Wornell, G.W., Williams, Z.M. & Brown, E.N. Feedback-controlled parallel point process filter for estimation of goal-directed movements from neural signals. *IEEE Trans. Neural Syst. Rehabil. Eng.* published online, doi:10.1109/TNSRE.2012.2221743 (2 October 2012).
18. Shanechi, M.M., Williams, Z.M., Wornell, G.W. & Brown, E.N. A brain-machine interface combining target and trajectory information using optimal feedback control. in *Computational and Systems Neuroscience (COSYNE) Meeting* (Salt Lake City, USA, 2011).
19. Kurata, K. Premotor cortex of monkeys: set- and movement-related activity reflecting amplitude and direction of wrist movements. *J. Neurophysiol.* **69**, 187–200 (1993).
20. Messier, J. & Kalaska, J.F. Covariation of primate dorsal premotor cell activity with direction and amplitude during a memorized-delay reaching task. *J. Neurophysiol.* **84**, 152–165 (2000).
21. Crammond, D.J. & Kalaska, J.F. Modulation of preparatory neuronal activity in dorsal premotor cortex due to stimulus-response compatibility. *J. Neurophysiol.* **71**, 1281–1284 (1994).
22. Boussaoud, D. & Bremmer, F. Gaze effects in the cerebral cortex: reference frames for space coding and action. *Exp. Brain Res.* **128**, 170–180 (1999).
23. Crammond, D.J. & Kalaska, J.F. Differential relation of discharge in primary motor cortex and premotor cortex to movements versus actively maintained postures during a reaching task. *Exp. Brain Res.* **108**, 45–61 (1996).
24. Crammond, D.J. & Kalaska, J.F. Prior information in motor and premotor cortex: activity during the delay period and effect on pre-movement activity. *J. Neurophysiol.* **84**, 986–1005 (2000).
25. Crutcher, M.D., Russo, G.S., Ye, S. & Backus, D.A. Target-, limb-, and context-dependent neural activity in the cingulate and supplementary motor areas of the monkey. *Exp. Brain Res.* **158**, 278–288 (2004).
26. Hocherman, S. & Wise, S.P. Effects of hand movement path on motor cortical activity in awake, behaving rhesus monkeys. *Exp. Brain Res.* **83**, 285–302 (1991).
27. Batista, A.P. & Andersen, R.A. The parietal reach region codes the next planned movement in a sequential reach task. *J. Neurophysiol.* **85**, 539–544 (2001).
28. Ninokura, Y., Mushiake, H. & Tanji, J. Representation of the temporal order of visual objects in the primate lateral prefrontal cortex. *J. Neurophysiol.* **89**, 2868–2873 (2003).
29. Tanji, J. & Shima, K. Role for supplementary motor area cells in planning several movements ahead. *Nature* **371**, 413–416 (1994).
30. Shima, K., Isoda, M., Mushiake, H. & Tanji, J. Categorization of behavioural sequences in the prefrontal cortex. *Nature* **445**, 315–318 (2007).
31. Shima, K. & Tanji, J. Neuronal activity in the supplementary and presupplementary motor areas for temporal organization of multiple movements. *J. Neurophysiol.* **84**, 2148–2160 (2000).
32. Baldauf, D., Cui, H. & Andersen, R.A. The posterior parietal cortex encodes in parallel both goals for double-reach sequences. *J. Neurosci.* **28**, 10081–10089 (2008).
33. Averbeck, B.B., Sohn, J.-W. & Lee, D. Activity in prefrontal cortex during dynamic selection of action sequences. *Nat. Neurosci.* **9**, 276–282 (2006).
34. Mushiake, H., Saito, N., Sakamoto, K., Itoyama, Y. & Tanji, J. Activity in the lateral prefrontal cortex reflects multiple steps of future events in action plans. *Neuron* **50**, 631–641 (2006).
35. Ohbayashi, M., Ohki, K. & Miyashita, Y. Conversion of working memory to motor sequence in the monkey premotor cortex. *Science* **301**, 233–236 (2003).
36. Kettner, R.E., Marcario, J.K. & Port, N.L. Control of remembered reaching sequences in monkey. II. Storage and preparation before movement in motor and premotor cortex. *Exp. Brain Res.* **112**, 347–358 (1996).
37. Lu, X. & Ashe, J. Anticipatory activity in primary motor cortex codes memorized movement sequences. *Neuron* **45**, 967–973 (2005).
38. Nakajima, T., Hosaka, R., Mushiake, H. & Tanji, J. Covert representation of second-next movement in the pre-supplementary motor area of monkeys. *J. Neurophysiol.* **101**, 1883–1889 (2009).
39. Averbeck, B.B., Chafee, M.V., Crowe, D.A. & Georgopoulos, A.P. Parallel processing of serial movements in prefrontal cortex. *Proc. Natl. Acad. Sci. USA* **99**, 13172–13177 (2002).
40. Saito, N., Mushiake, H., Sakamoto, K., Itoyama, Y. & Tanji, J. Representation of immediate and final behavioral goals in the monkey prefrontal cortex during an instructed delay period. *Cereb. Cortex* **15**, 1535–1546 (2005).
41. Mushiake, H., Inase, M. & Tanji, J. Selective coding of motor sequence in the supplementary motor area of the monkey cerebral cortex. *Exp. Brain Res.* **82**, 208–210 (1990).
42. Smith, A.C. *et al.* State-space algorithms for estimating spike rate functions. *Comput. Intell. Neurosci.* published online, doi:10.1155/2010/426539 (5 November 2009).
43. Tanji, J. Sequential organization of multiple movements: involvement of cortical motor areas. *Annu. Rev. Neurosci.* **24**, 631–651 (2001).
44. Cisek, P. & Kalaska, J.F. Neural correlates of reaching decisions in dorsal premotor cortex: specification of multiple direction choices and final selection of action. *Neuron* **45**, 801–814 (2005).
45. Hoshi, E. & Tanji, J. Integration of target and body-part information in the premotor cortex when planning action. *Nature* **408**, 466–470 (2000).
46. Hoshi, E. & Tanji, J. Contrasting neuronal activity in the dorsal and ventral premotor areas during preparation to reach. *J. Neurophysiol.* **87**, 1123–1128 (2002).
47. Hoshi, E. & Tanji, J. Differential involvement of neurons in the dorsal and ventral premotor cortex during processing of visual signals for action planning. *J. Neurophysiol.* **95**, 3596–3616 (2006).
48. Shima, K. & Tanji, J. Both supplementary and presupplementary motor areas are crucial for the temporal organization of multiple movements. *J. Neurophysiol.* **80**, 3247–3260 (1998).

ONLINE METHODS

Behavioral tasks. Two adult rhesus monkeys (*Macaca mulatta*) were trained to perform a working memory sequential delayed motor task. Monkeys were first sequentially presented with two distinct target locations on a screen, which were randomly selected in each trial, and then had to move a cursor to each in order using a joystick (dual-target task; **Fig. 1a**). After an initial presentation of a blank screen, two targets were sequentially presented, each of which could randomly take on one of four possible spatial locations: up, down, right or left. To ensure that the two target locations were distinct, the motor sequence was chosen at random from a total of 12 possible sequences such that all possible combinations of the two target locations, excluding the ones with repeated locations, were shown. Targets were displayed for 500 ms each and were interleaved by a 300-ms interval during which a blank screen was shown. After the end of second target presentation, there was an additional blank screen variable delay of 550–850 ms (the working memory period), after which the first go cue signal appeared. After this, the monkeys were required to move a cursor from the center of the screen to the first remembered target. After reaching the target, they were required to return the joystick to the center and then wait for a second go cue to appear after an additional 500-ms delay interval. Once the second go cue appeared, the monkeys were allowed to move the cursor from the center of the screen to the second remembered target. They received a juice reward if they correctly moved to the two instructed targets.

Dual-target and single-target tasks. To examine the effect of adding information about a new target to working memory, it was necessary to disambiguate the process of holding information in working memory from that of adding information to it. To do this, primates performed randomly interleaved dual-target and single-target trials in a subset of sessions. In the dual-target trials, described above, the primates were sequentially presented with two targets and then a blank screen delay. The time delay from the end of the first target presentation to the first go cue was therefore 1,350–1,650 ms. In the single-target trials, in comparison, the primates were presented with only the first target and had to keep this single target in working memory for the same total 1,350- to 1,650-ms time duration as in the dual-target trials. However, they were not presented with a second target and only shown a blank screen until the go cue.

Neurophysiologic recordings. All procedures were performed under Institutional Animal Care and Use Committee–approved guidelines and were approved by the Massachusetts General Hospital institutional review board. Before the recordings, multiple (up to six) planar silicone multielectrode arrays (NeuroNexus Technologies Inc., MI) were surgically implanted in each monkey. Each of the implanted arrays contained four shanks horizontally spaced 400 μm apart. Every shank was 4 mm long and contained eight electrode contacts, each vertically spaced 200 μm apart for a total of 32 contacts per electrode array. Hence, the electrode contacts themselves spanned the bottom 1.6 mm of the shank. We advanced the electrodes approximately 2 mm in depth. The electrode arrays were inserted into the cortex manually using microscope magnification. A craniotomy was placed over the premotor cortex under stereotactic guidance (David Kopf Instruments, CA). The multielectrode arrays were separately implanted into the PMd and supplementary motor areas (**Supplementary Fig. 10**). The electrode lead of each array was secured to the skull and attached to female connectors with the aid of titanium miniscrews and dental acrylic. Confirmation of the electrode positions was done in both monkeys by direct visual inspection of the sulcal and gyral pattern through the craniotomy. Additional postmortem confirmation of the electrode positions was made in one monkey (the second monkey is still performing experiments). Recordings began 2 weeks after surgical recovery. A Plexon multichannel acquisition processor was used to amplify and band-pass filter the neuronal signals (150 Hz to 8 kHz; one-pole low cut and three-pole high cut with 1,000× gain; Plexon Inc., TX). Shielded cabling carried the signals from the electrode array to a set of six 16-channel amplifiers. Signals were then digitized at 40 kHz and processed to extract action potentials in real time by the Plexon workstation. Classification of the action potential waveforms was performed using template matching and principle component analysis on the basis of waveform parameters. Only single, well-isolated units with identifiable waveform shapes and adequate refractory periods (less than 1% of spikes within a 1-ms interval) were used for the online experiments and offline analysis. No multiunit activity was used.

Model construction. For the analysis of standard recording sessions, we modeled the activity of each neuron under any given sequence as an inhomogeneous Poisson process whose likelihood function is given by[49,50]

$$p(N^c_{1:K} \mid S_i) = \prod_{k=1}^{K} (\lambda_c(k \mid S_i)\Delta)^{N^c_k} \exp(-\lambda_c(k \mid S_i)\Delta) \qquad i = 1:12 \qquad (1)$$

where Δ is the time increment taken to be small enough to contain at most one spike, N^c_k is the binary spike event of the c^{th} neuron in the time interval $[(k-1)\Delta, k\Delta]$, $\lambda_c(k|S_i)$ is its instantaneous firing rate in that interval, S_i is the i^{th} sequence, and K is the total number of bins in a duration $K\Delta$. We took $\Delta = 5$ ms as the bin width of the spikes. By building the neuronal models under each sequence separately in the dual-target task, we avoided making any a priori assumptions about whether the cells encode individual targets or combined sequences. For each sequence and neuron, we needed to estimate the firing rate $\lambda_c(k|S_i)$ using the neuronal data observed. To do so, we used a state-space approach using the expectation-maximization algorithm[42,51,52] (**Supplementary Modeling**). After fitting the models, we validated them using the χ^2 goodness-of-fit test on the data[42] and confirmed that they fitted the data well ($P > 0.7$ for all cells in all sessions).

Maximum-likelihood decoder. Once the models were fitted, a maximum-likelihood decoder was used to decode the intended sequence on the basis of the neuronal activity in any period of interest. A maximum-likelihood decoder is the optimal decoder in the sense of maximizing accuracy (the percentage of trials in which the combined sequence is decoded correctly when the sequences are equally likely to be presented, as was the case in our experiments). The decoder finds the likelihood of observing the population neuronal data under each sequence and selects the sequence with the highest likelihood as its prediction. Using the likelihood model in (1) and assuming that neurons are conditionally independent given the sequence, the population likelihood under any sequence is given by

$$p(N^{1:C}_{1:K} \mid S_i) = \prod_{c=1}^{C} \prod_{k=1}^{K} (\lambda_c(k \mid S_i)\Delta)^{N^c_k} \exp(-\lambda_c(k \mid S_i)\Delta) \qquad i = 1:12$$

where K is the total number of bins in any period of interest during the trial, C is the total number of neurons, and $\lambda_c(k|S_i)$ for k=1,…,K and c=1,…,C is the estimate of the firing rate. The predicted sequence, $\hat{S}$, is thus given by

$$\hat{S} = \arg\max_{S_i} p(N^{1:C}_{1:K} \mid S_i)$$

To find the sequence decoding accuracy of a single cell, the maximum-likelihood decoder uses only that cell's spiking activity to decode the sequence (**Fig. 5** and **Supplementary Fig. 5**). The decoder also outputs the posterior probability of each sequence, which is the probability that it is the correct one after the neuronal observations:

$$p(S_i \mid N^{1:C}_{1:K}) = \frac{p(N^{1:C}_{1:K} \mid S_i)}{\sum_i p(N^{1:C}_{1:K} \mid S_i)} \qquad i = 1, \cdots, 12$$

To dissociate the decoding accuracy of the first and second targets, denoted by T_1 and T_2, the decoder also outputs their predictions on the basis of the neuronal activity. To do so, the decoder finds their posterior probabilities, $p(T_1 = l_1 \mid N^{1:C}_{1:K})$ and $p(T_2 = l_2 \mid N^{1:C}_{1:K})$, for all possible spatial locations, l_1 and l_2, by summing over the posterior probability of the sequences that have these spatial locations as their first or second targets. The decoder then picks the spatial location with the highest first target posterior (that is equivalent in our design to picking the first target location that maximizes the population likelihood) as its first target prediction and similarly does so for the second target.

Comparison of the first-target decoding accuracies in the single-target and dual-target trials. To find the first-target decoding accuracy in the single-target trials, we modeled the activity of each neuron under any given single target location as an inhomogeneous Poisson process, which was fitted using the expectation-maximization procedure. We then performed the maximum-likelihood decoding analysis using leave-one-out cross-validation on the single-target trials. To make the comparison, for the dual-target trials we constructed

two models, one for the first target and one for the second target, and then performed the decoding analysis for each target separately.

Determining the number of cells required to achieve the population accuracy. We found the number of cells required to achieve a given percentage of the population accuracy by first sorting them in each session on the basis of their single neuron sequence accuracies and then performing the decoding analysis in that session for different number of cells in descending order.

BMI model training. In each BMI recording session, the monkeys first performed the dual-target task using a joystick (training session) during which models were constructed for the neuronal activity during an 800-ms time window before presentation of the go cue. This window length was chosen because in the standard dual-target sessions it was sufficient to achieve better than 95% of the (maximum) sequence accuracy possible when using the entire window starting from second target presentation until the go cue (**Supplementary Fig. 1b**). We modeled the activity of each neuron in this window under any sequence as a homogeneous Poisson process (point process with constant rate) instead of an inhomogeneous process to make the model construction faster for the BMI experiments. Hence, using (1), the likelihood function for the spiking activity of neuron c under any of the sequences, S_i, was modeled as[49,50]

$$p(N^c_{1:K} \mid S_i) = \prod_{k=1}^{K} (\lambda_c(S_i)\Delta)^{N^c_k} \exp(-\lambda_c(S_i)\Delta)$$

where $\lambda_c(S_i)$ denotes the fitted firing rate of that neuron in the 800-ms window for sequence S_i, and $K = 800/\Delta$ is the total number of bins in this period with bin width $\Delta = 5$ ms. The firing rates were fitted using maximum-likelihood parameter estimation. The task involved either four (both monkeys) or eight (monkey P) sequences. The four-sequence task consisted of either up-right, up-left, down-right, down-left or left-up, left-down, right-up, right-down. The eight-sequence task consisted of the union of the sequences in the two four-sequence tasks.

The training sessions were followed by the real-time BMI sessions in which these trained Poisson models were used to predict the sequence using the maximum-likelihood decoder.

Concurrent online predictions and movement execution in the BMI. After the training sessions, the monkeys performed the same task as before. However, this time cursor position was controlled by target predictions made by the maximum-likelihood decoder rather than the joystick. During the real-time BMI experiments, individual spike timings of all cells within the population were continuously recorded at a 40-kHz resolution by the Plexon multichannel acquisition processor. Each recorded spike was then transmitted through an ethernet port to a separate computer running a Matlab routine in real time. For each real-time trial, the Matlab routine then used the maximum-likelihood decoder to calculate the likelihood of the population spiking activity during the 800-ms time window before the go cue, $N^{1:C}_{1:K}$, under each sequence, S_i. This likelihood was calculated on the basis of the trained Poisson models and assuming neurons were independent conditioned on the sequence. Hence, the population likelihood for each sequence was found as

$$p(N^{1:C}_{1:K} \mid S_i) = \prod_{c=1}^{C}\prod_{k=1}^{K} (\lambda_c(S_i)\Delta)^{N^c_k} \exp(-\lambda_c(S_i)\Delta)$$

The maximum-likelihood decoder then outputted the sequence under which the population likelihood was maximized as the decoded sequence.

On the basis of the sequence decoded, a second Matlab routine running on the same computer then activated an analog output channel on the National Instruments Data Acquisition Input/Output (NI DAQ I/O) interface to go from 0 V to either +5 V or −5V for 500 ms. The voltage line was connected to a second NI DAQ I/O input channel located on a third computer running the behavioral program. Depending on the voltage received, the cursor displayed in the middle of the screen moved in a straight line to one of the four possible target locations (for example, +5 V in I/O channel 1 corresponded to a cursor location within the top target). This process then repeated for the second decoded target after another artificially introduced time delay. The time delays in the two generated movements were selected to be similar to those that the monkeys normally experienced when performing the standard task using a joystick. However, the NI DAQ could, in principle, generate the two movements in as little as a few milliseconds apart.

Behavior and prediction errors. Because the primates did not perform the dual-target working memory task with 100% behavioral accuracy, some of the BMI errors were caused by behavioral errors (for example, the monkey not remembering the correct sequence during working memory) as opposed to decoder errors. Hence, a more relevant accuracy number for the performance of the BMI could be the sequence accuracy obtained during the training session using leave-one-out cross-validation. This is because in the cross-validation analysis, we calculated the accuracy by comparing the decoded sequence with the sequence the monkeys actually selected after the go cue. For the BMI sessions, however, we compared the decoded sequence to the instructed sequence to find the accuracy. We therefore tested whether, after taking into account the primates' natural error rates, the accuracy during training sessions would be close to the BMI accuracy. Denoting the behavioral accuracy of the monkeys by P_b and the decoder accuracy found from the training session by P_t, we can calculate what the accuracy of selecting the instructed sequence would be after taking into account the behavioral errors. Denoting the resulting accuracy by P_f, we have that

$$P_f = P_b P_t + (1-P_b)(1-P_t)\times\frac{1}{S-1}$$

In other words, when the monkey and the decoder are both correct, the instructed sequence is selected. However, if the monkey is incorrect and the decoder is also incorrect in decoding the monkey's intended sequence, the probability of the decoder selecting the correct instructed sequence by random chance is 1/(S−1). We can find the mean and s.e.m. of P_f from those of P_b and P_t, assuming P_b and P_t are independent[53], and then compare it with the BMI accuracy.

49. Brown, E.N., Barbieri, R., Eden, U.T. & Frank, L.M. Likelihood methods for neural data analysis. in *Computational Neuroscience: A Comprehensive Approach* (ed. Feng, J.) 253–286 (CRC Press, 2003).
50. Truccolo, W., Eden, U.T., Fellows, M.R., Donoghue, J.P. & Brown, E.N. A point process framework for relating neural spiking activity to spiking history, neural ensemble, and extrinsic covariate effects. *J. Neurophysiol.* **93**, 1074–1089 (2005).
51. Smith, A.C. & Brown, E.N. Estimating a state-space model from point process observations. *Neural Comput.* **15**, 965–991 (2003).
52. Dempster, A.P., Laird, N.M. & Rubin, D.B. Maximum likelihood from incomplete data via the EM algorithm. *J. Royal Stat. Soc., Series B* **39**, 1–38 (1977).
53. Goodman, L.A. On the exact variance of products. *J. Am. Stat. Assoc.* **55**, 708–713 (1960).

doi:10.1038/nn.3250